Video Title	Year / Authors / Publication or other source	Experimental details	Description	Relevant chapter in “Liquid Cell Electron Microscopy”	Thumbnail / Video link
Dendritic copper growth	2002: M. J. Williamson, *Investigations of materials issues in advanced interconnect structures*, Ph. D. Thesis, University of Virginia	Hitachi H-9000; 300kV; bright field imaging; 30 frames per second. Home-built “IBM Liquid Cell” with one Au and one Cu electrode	Electrochemical growth at the tip of a micrometers-long Cu dendrite	10	Dendritic-copper-growth.avi 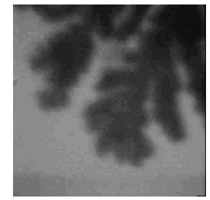
Galvanostatic copper deposition and stripping	2003: M. J. Williamson, R. M. Tromp, P. M. Vereecken, R. Hull and F. M. Ross, *Dynamic electron microscopy in liquid environments*, Nature Materials **2**, 532-536. Reprinted with permission.	Hitachi H-9000; 300kV; bright field imaging; 30 frames per second. Home-built “IBM Liquid Cell” with one Au and one Cu electrode. Horizontal field of view 6.3µm; speeded up x2	Electrochemical nucleation and stripping of copper islands on Au at constant current density 50 mA/cm^2, 0.3M $CuSO_4$ electrolyte	10	Galvanostatic-copper.mov 
Potentiostatic copper deposition	2006: A. Radisic, P. M. Vereecken, J. B. Hannon, P. C. Searson and F. M. Ross, *Quantifying electrochemical nucleation and growth mechanisms from real-time kinetic data*. Nano Letters **6**, 238-242. Reprinted with permission. Copyright (2006) American	Hitachi H-9000; 300kV; bright field imaging; 30 frames per second. Home-built 3-terminal “IBM Liquid Cell” with Au working and counter electrodes and Cu reference electrode. Horizontal field of view 1.8µm; speeded up x1.5.	Electrochemical nucleation of copper islands on Au at constant potential -0.6V, 0.1M $CuSO_4$ + 0.18M H_2SO_4 electrolyte; Shows ability to correlate images with electrochemical parameters.	10	Potentiostatic-copper.mov 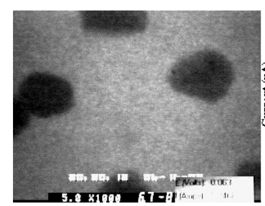 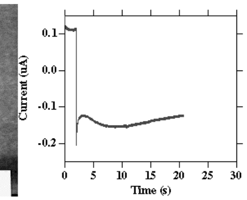

	Chemical Society.				
Lithiation of crystalline SnO_2 nanowire	2010: J. Y. Huang, L. Zhong, C. M. Wang, J. P. Sullivan, W. Xu, L. Q. Zhang, S. X. Mao, N. S. Hudak, X. H. Liu, A. Subramanian, H. Fan, L. Qi, A. Kushima and J. Li, *In Situ Observation of the Electrochemical Lithiation of a Single SnO_2 Nanowire Electrode,* Science, **330**, 1515-1520. Reprinted with permission. Copyright (2010), AAAS	FEI Tecnai; 300kV; bright field imaging; 2 frames per second. Open cell built in a Nanofactory Nanomanipulator with Si as anode, $LiCoO_2$ as cathode and ionic liquid based electrolyte. Scale bar 200nm. Video speeded up 33x.	Injection of Li ions (i. e., charging) into crystalline SnO_2 drives a transformation into amorphous $Li_xSn_yO_z$ and a volume expansion of ~ 200%. The shape and volume change is visible.	3	huang-SnO2-lithiation-volumechange.avi 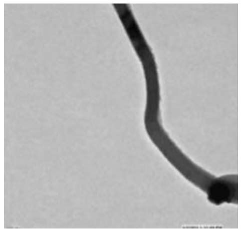
Reaction front during lithiation of crystalline SnO_2 nanowire	2010: J. Y. Huang, L. Zhong, C. M. Wang, J. P. Sullivan, W. Xu, L. Q. Zhang, S. X. Mao, N. S. Hudak, X. H. Liu, A. Subramanian, H. Fan, L. Qi, A. Kushima and J. Li, *In Situ Observation of the Electrochemical Lithiation of a Single SnO_2 Nanowire Electrode,* Science, **330**, 1515-1520. Reprinted with permission. Copyright (2010), AAAS	FEI Tecnai; 300kV; bright field imaging; 2 frames per second. Open cell built in a Nanofactory Nanomanipulator with Si as anode, $LiCoO_2$ as cathode and ionic liquid based electrolyte. Scale bar 100nm. Video speeded up 30x.	Injection of Li ions (i. e., charging) into crystalline SnO_2 drives a transformation into amorphous $Li_xSn_yO_z$ and a volume expansion of ~ 200%. Defects at the reaction front are visible.	3	huang-SnO2-lithiation-reactionfront.avi 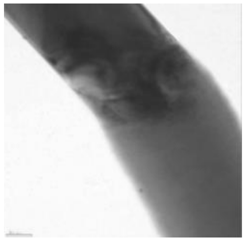
Assembly of silica spheres	2011: M. Suga, H. Nishiyama, Y. Konyuba, et al., *The atmospheric scanning electron microscope with open sample space observes*	JEOL Clairscope (Atmospheric SEM), JASM-6200, 30keV, 0.6 sec per frame. BSE contrast. Horizontal field of view and	Beam-induced assembly of silica spheres, 1um diameter, in contact with Si_xN_y window. At magnification 5kx random motion is visible. When	5	Suga-silica-sphere-assembly.mov

	dynamic phenomena in liquid or gas, Ultramicroscopy **111**, 1650-1658. Reprinted with permission. Copyright © 2011 Elsevier B.V.	current density were 12 μm (9 pA/μm^2) then then 6 μm (36 pA/μm^2) then 12 μm.	increased to 10kx the particles self-organized. Back at 5kx the cluster dispersed.		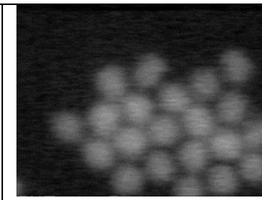
Motion of aggregated protein balls	2011: M. Suga, H. Nishiyama, Y. Konyuba, et al., *The atmospheric scanning electron microscope with open sample space observes dynamic phenomena in liquid or gas,* Ultramicroscopy **111**, 1650-1658. Reprinted with permission. Copyright © 2011 Elsevier B.V.	JEOL Clairscope (Atmospheric SEM), JASM-6200, 30keV, 0.6 sec per frame. BSE contrast. Horizontal field of view 3 μm.	Motion and close packing of ~200 nm aggregated protein balls created by fixing MIP-1α protein (7.8 kDa) with glutaraldehyde then staining with phosphotungstic acid.	5	Suga-protein-aggregation.mov 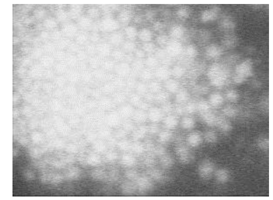
Crystallization during evaporation	2011: M. Suga, H. Nishiyama, Y. Konyuba, et al., *The atmospheric scanning electron microscope with open sample space observes dynamic phenomena in liquid or gas,* Ultramicroscopy **111**, 1650-1658. Reprinted with permission. Copyright © 2011 Elsevier B.V.	JEOL Clairscope (Atmospheric SEM), JASM-6200, 30keV, 40 pA, 0.6 sec per frame, 1000x magnification. BSE contrast. Horizontal field of view 100 μm.	Evaporation-induced crystallization of PBS (Phosphor Buffer Saline) solution.	5	Suga-PBS-crystallization.mov 
Electrochemical deposition of Au	2011: M. Suga, H. Nishiyama, Y. Konyuba, et al., *The atmospheric scanning electron*	JEOL Clairscope (Atmospheric SEM), JASM-6200, 30keV, 0.6 sec per frame, 5000x	Deposition of Au derived from dissolution of CE. Saturated NaCl, 2.1V applied between	5, 10	Suga-Au-electrodeposition.mov

	microscope with open sample space observes dynamic phenomena in liquid or gas, Ultramicroscopy **111**, 1650-1658. Reprinted with permission. Copyright © 2011 Elsevier B.V.	magnification, BSE contrast. Horizontal field of view 20 μm. Two electrodes, 100nm thick Au on 30nm Ti; separation 100 μm.	electrodes.		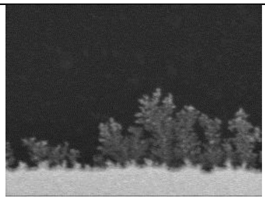
Bubble formation induced by Joule heating	2011: E.R. White, M. Mecklenburg, S.B. Singer, S. Aloni, B.C. Regan, *Imaging Nanobubbles in Water with Scanning Transmission Electron Microscopy*, Appl. Phys. Express **4**, 055201-1.	FEI Titan 80-300 STEM/TEM; 300 kV. Home-built liquid cell with an e-beam deposited Pt heater wire in water. Field of view 10 μm.	Vapor bubbles in water induced by applying 500 μW pulses to a Pt heater.	6, 7, 13	Regan-jouleheating.avi 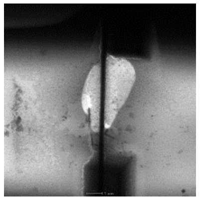
Beam-driven particle motion and bubble formation	2012: E.R. White, M. Mecklenburg, B. Shevitski, S.B. Singer, B.C. Regan, *Charged nanoparticle dynamics in water induced by scanning transmission electron microscopy*, Langmuir **28**, 3695-3698.	FEI Titan 80-300 STEM/TEM; 300 kV. Home-built liquid cell with e-beam deposited Pt nanoparticles in water. Field of view 3 μm.	Driven motion of Pt nanoparticles and bubble generation in a liquid cell subject to a 240 pA STEM beam current.	7, 9, 13	Regan-beaminducedmotion.avi 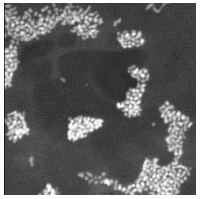
Lead dendrite growth and stripping	2012: E.R. White, S.B. Singer, V. Augustyn, W.A. Hubbard, M. Mecklenburg, B. Dunn, B.C. Regan, *In Situ*	FEI Titan 80-300 STEM/TEM; 300 kV. Home-built liquid cell with Au electrodes and a saturated solution of	Repeated growth and shrinkage of lead dendrites on a gold electrode subject to step changes in the potential.	10	Regan-Pbdendrite.avi

	Transmission Electron Microscopy of Lead Dendrites and Lead Ions in Aqueous Solution, ACS Nano **6**, 6308-6317.	$Pb(NO_3)_2$ in water. Field of view 6 μm.			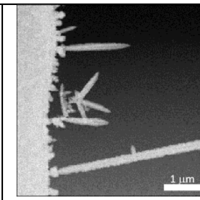
Lithiation and pulverization of crystalline silicon particles	2012: M. T. McDowell , I. Ryu , S. W. Lee , C. M. Wang , W. D. Nix and Y. Cui, *Studying the Kinetics of Crystalline Silicon Nanoparticle Lithiation with In Situ Transmission Electron Microscopy,* Adv. Mater. **24**, 6034–6041. Reprinted with permission. Copyright (2012), Wiley.	FEI Titan; 300kV; bright field imaging; 30 frames per second. Open cell built in a Nanofactory Nanomanipulator with Si as anode, $LiCoO_2$ as cathode and ionic liquid based electrolyte. Scale bar 100nm; video speeded up 16x.	Injection of Li ions (i. e., charging) into crystalline Si drives a transformation into amorphous Li_xSi and a volume expansion of ~ 300%. Stress associated with the volume change pulverizes the large particles.	3	Wang-Si-pulverization.avi 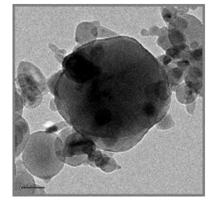
Faceted silver nanoparticle growth	2012: T. J. Woehl, J. E. Evans, I. Arslan, W. D. Ristenpart and N. D. Browning, *Direct in Situ Determination of the Mechanisms Controlling Nanoparticle Nucleation and Growth*, ACS Nano **6**, 8599-8610. Reprinted with permission. Copyright (2012) American Chemical Society.	Cs-corrected JEOL 2100F; 200 kV; 7 pA beam current; bright field STEM; 1 frame per second. Hummingbird Scientific liquid cell	Radiolytic reduction of silver nitrate into monovalent silver species, which nucleate and grow into faceted silver nanocrystals on the Si_xN_y membrane. FOV is 1.6 x 1.6µm.	9	Woehl-SilverNanoparticleGrowth.avi 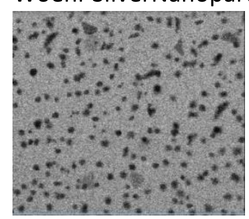

Motion of Au nanorods	2013: M. J. Dukes, B. W. Jacobs, D. G. Morgan, H. Hegde, and D. F. Kelly, *Visualizing nanoparticle mobility in liquid at atomic resolution*, Chem. Comm. **49**, 3007-3009. Reprinted with permission.	FEI Tecnai; 120kV; bright field imaging; 10 frames per second. Poseidon liquid specimen holder (Protochips, Inc.) Horizonal field of view ~1 µm; speeded up x4	Nanoscale tidal waves cause PVP-coated gold nanorods to move in solution.	17	Kelly-Au-rod-motion.mov 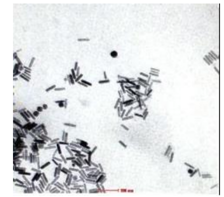
Sodiation of crystalline SnO_2 nanowire	2013: M. Gu, A. Kushima, Y. Shao, J.-G. Zhang, J. Liu, N. D. Browning, J. Li and C. M. Wang, *Probing the Failure Mechanism of SnO_2 Nanowires for Sodium-Ion Batteries,* Nano Lett. **13**, 5203–5211, Reprinted with permission. Copyright (2013) American Chemical Society.	FEI Titan; 300kV; bright field imaging; 30 frames per second. Open cell built in a Nanofactory Nanomanipulator with Na as anode, SnO_2 as cathode and sodium oxide as electrolyte. Nanowire diameter 200nm. Video speeded up 16x.	Injection of Na ions (i. e., charging a sodium ion battery) into crystalline SnO_2 drives transformation to amorphous $Na_xSn_yO_z$ and volume expansion	3	Wang-SnO2-sodiation.avi 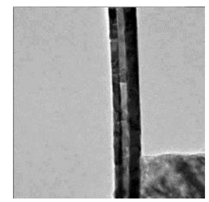
Lithiation of silicon particle in hollow carbon	2014: C. M. Wang unpublished data	FEI Titan; 300kV; bright field imaging; 30 frames per second. Open cell built in a Nanofactory Nanomanipulator with Si as anode, $LiCoO_2$ as cathode, and ionic liquid based electrolyte. Video speeded up 16x.	Lithiation of Si nanoparticle enclosed in hollow carbon shell, demonstrating that the carbon shell can act as a buffer layer to separate the Si from the liquid electrolyte	3	Wang-Si-lithiation-with-carbon-shell.avi 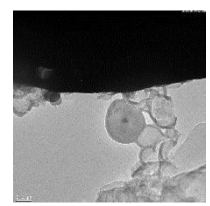
Lithiation of silicon particle in hollow carbon	2014: C. M. Wang unpublished data	FEI Titan; 300kV; HRTEM; 30 frames per second. Open cell built in a Nanofactory	HRTEM image showing the lithiation of Si and crystalline to amorphous transition	3	Wang-Si-lithiation-HRTEM.avi

		Nanomanipulator with Si as cathode, Li as anode and Li_2O as electrolyte. Scale bar 2nm. Video speeded up 8x.			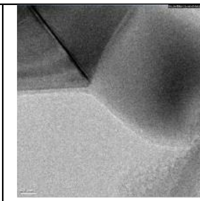
Hydrogen bubble nucleation	2014: J. M. Grogan, N. M. Schneider, F. M. Ross and H. H. Bau, *Bubble and pattern formation in liquid induced by an electron beam*, Nano Letters **14**, 359-364. Reprinted with permission. Copyright (2014) American Chemical Society.	Hitachi H-9000; 300kV; bright field imaging; 30 frames per second. UPenn "Nanoaquarium"	Radiolytic formation of hydrogen bubbles that nucleate at a defect on the Si_xN_y membrane. Water with trace CTAB; current density <20 A/m^2. Horizontal field of view 0.98µm; speeded up x2.	7	Hydrogen-bubble-nucleation.avi 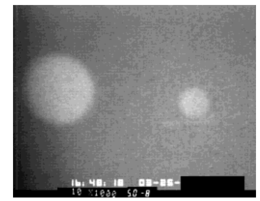
Assembly of gold nanoparticles into 1D chains	2015: T. J. Woehl and T. Prozorov, *The Mechanisms for Nanoparticle Surface Diffusion and Chain Self-Assembly Determined from Real-Time Nanoscale Kinetics in Liquid*, Journal of Physical Chemistry C **119**, 21261-21269. Reprinted with permission. Copyright (2015) American Chemical Society.	FEI Tecnai F20; 200 kV; ADF STEM; 2 frames per second. Hummingbird Scientific liquid cell	Electron beam induced diffusion and assembly of gold nanoparticles into 1D chains and branched structures. FOV is 1.2 x 1.2µm.	9, 23	Woehl-GoldNanoparticleAssembly.avi 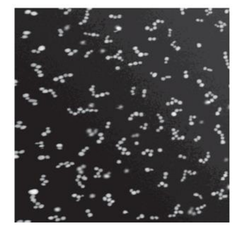
Active rotavirus particles in	2015: A. C. Varano, A. Rahimi, M. J. Dukes, S.	FEI Tecnai; 120kV; bright field imaging; 4	Transcriptionally-active rotavirus particles were	17	Kelly-transscribingvirus.mov

solution	Poelzing, S. M. McDonald and D. F. Kelly. *Visualizing virus particle mobility in liquid at the nanoscale*, Chem. Comm. **51**, 16176-16179. Reprinted with permission.	frames per second. Poseidon liquid specimen holder (Protochips, Inc.)	subjected to a density threshold function, followed by contour mapping to see movements in the internal genetic material. Real-time acquisition.		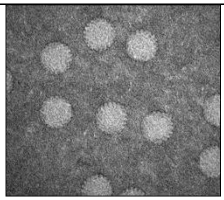
Potentiostatic silver plating and stripping	2015: J. Velmurugan, A. Stevanovic, F. Yi, D. LaVan and A. Kolmakov (unpublished)	JEOL JSM-7800F, Everhart-Thornley detector; home built NIST SEM gas/liquid cell; 50nm Si_xN_y membrane; 0.1 M $AgNO_3$ solution. E_{beam}= 5 keV, beam current ~100 pA	Ag dendrites growth upon application of constant potential -0.6V to Pt electrode and strip off at opposite potential. Speeded up x2.	4, 11	Kolmakov-Agdendrites.mp4 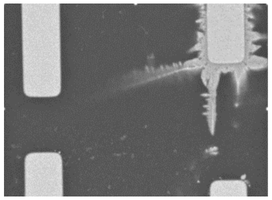
CsI crystals growth	2016: A. Kolmakov (unpublished)	JEOL JSM-7800F, Everhart-Thornley electron detector; Bilayer graphene multichannel liquid cell. E_{beam}= 5 keV; beam current ~100 pA	Beam induced CsI crystal nucleation and growth from CsI aqueous solution. Circles are individual 5 micron wide channels filled with solution and capped with bilayer graphene. The matrix is made of silica covered with Au film.	4, 7, 10	Kolmakov-CsI.mp4 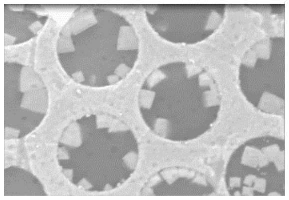
Etching of Au nanorods	2016: X. Ye, M. R. Jones, L. B. Frechette, Q. Chen, A. S. Powers, P. Ercius, G. Dunn, G. M. Rotskoff, S. C. Nguyen, V. P. Adiga, A.	FEI Tecnai G2 20 S-TWIN TEM with Gatan Orius SC200 CCD camera; 200kV; 2.5 frames per second, dose rate 217 e/Å^2.s.	Simultaneous dissolution of a regular and blunted Au nanorod. The electron beam is used to control the Au dissolution in a redox environment (ferric	7, 9	Adiga-etching-rods.mp4

	Zettl, E. Rabani, P. L. Geissler and A. P. Alivisatos, *Single-particle mapping of nonequilibrium nanocrystal transformations,* Science **354**, 874-877. Reprinted with permission.	Graphene liquid cell.	chloride solution), providing information on shape stability.		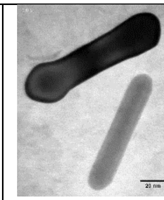
Etching of Au nanocube	2016: X. Ye, M. R. Jones, L. B. Frechette, Q. Chen, A. S. Powers, P. Ercius, G. Dunn, G. M. Rotskoff, S. C. Nguyen, V. P. Adiga, A. Zettl, E. Rabani, P. L. Geissler and A. P. Alivisatos, *Single-particle mapping of nonequilibrium nanocrystal transformations,* Science **354**, 874-877. Reprinted with permission.	FEI Tecnai G2 20 S-TWIN TEM with Gatan Orius SC200 CCD camera; 200kV; 2.5 frames per second, dose rate 86 e/Å^2.s. Graphene liquid cell.	Dissolution of an Au nanocube exhibiting the tetrahexahedron transient intermediate shape. The electron beam is used to control the Au dissolution in a redox environment (ferric chloride solution).	7, 9	Adiga-etching-cube.mp4